

# Supplementary Materials for

## Identification of nonhistone substrates of the lysine methyltransferase PRDM9

Jocelyne N. Hanquier<sup>1,2</sup>, Kenidi Sanders<sup>1,3</sup>, Christine A. Berryhill<sup>1</sup>, Firoj K. Sahoo<sup>5</sup>, Andy Hudmon<sup>5</sup>, Jonah Z. Vilseck<sup>1,3,4</sup>, Evan M. Cornett<sup>1-4,\*</sup>

<sup>1</sup>Department of Biochemistry and Molecular Biology, <sup>2</sup>Stark Neuroscience Research Institute, <sup>3</sup>Melvin and Bren Simon Comprehensive Cancer Center, <sup>4</sup>Center for Computational Biology and Bioinformatics, Indiana University School of Medicine, Indianapolis, IN 46202, U.S.A.; <sup>5</sup>Department of Medicinal Chemistry and Molecular Pharmacology, College of Pharmacy, Purdue University, West Lafayette, IN 47907 U.S.A.

### The PDF file includes:

Supplementary Fig. 1: Analysis of PRDM9 substrate selectivity using a K-OPL

Supplementary Fig. 2: Evaluation of the “pan”-ness of pan-specific anti-lysine methyl antibodies.

Supplementary Fig. 3 Additional MS $\lambda$ D trajectory analyses of PRDM9 substrate selectivity.

Supplementary Fig. 4: Domain maps of putative PRDM9 non-histone substrates and *in vitro* methyltransferase assays using recombinant proteins.

### Other Supplementary Material includes the following:

Supplementary Table 1: Score of all 7-mer motifs in human proteins based on PRDM9 K-OPL data.

Supplementary Table 2: Layout of peptide spot array (Figure 4B)

Supplementary Table 3: Characterization of peptide spot array substrates.

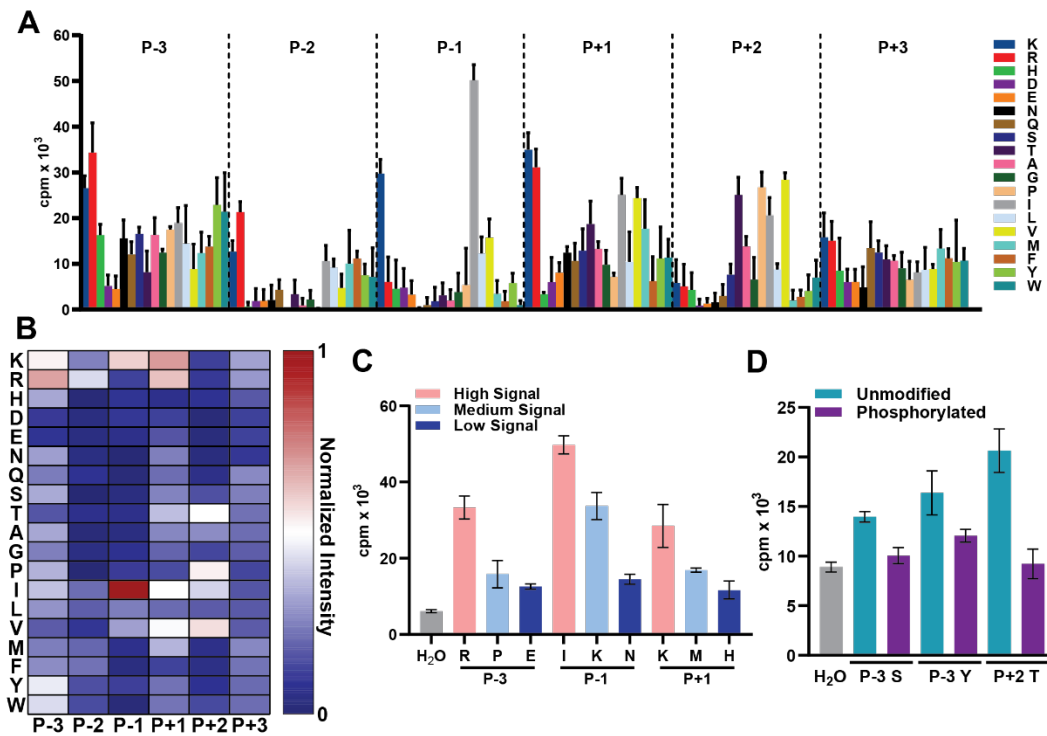


**Figure S1. Analysis of PRDM9 substrate selectivity using a K-OPL.** *A*, Data for PRDM9 K-OPL selectivity profile showing average signal for reactions with each K-OPL set (n=3). *B*, Heatmap normalized globally to the set with the highest signal. *C*, Validation of PRDM9 K-OPL selectivity profile on select K-OPL sets (n=2). *D*, PRDM9 reactions on phosphorylated K-OPL sets (n=3). Bar graphs display mean  $\pm$ SD.

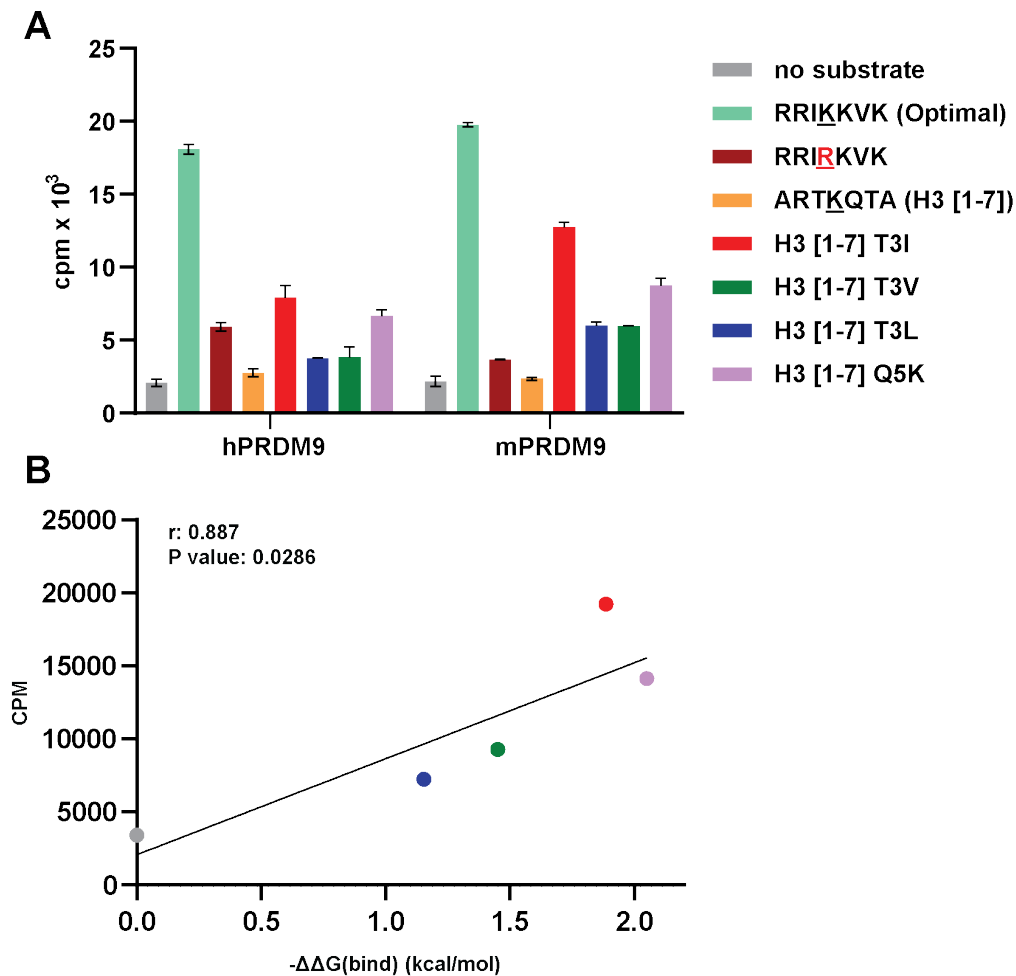


**Figure S2. Analysis of PRDM9 substrate selectivity using a K-OPL** *A*, Comparison of human PRDM9 and mouse Prdm9 on peptide substrates shows the highly homologous PR/SET domain have the same substrate selectivity on peptides used in this study. Graph depicts mean ( $n=2$ )  $\pm$ SD signal from scintillation proximity methyltransferase assays (SPA) with biotin labeled peptides. *B*, Correlation of changes in relative binding free energies determined from MSAD for H3 peptides substituted at critical positions with experimental changes in methyltransferase activity for PRDM9. On-tailed Pearson ( $r$ ) correlation was calculated using GraphPad Prism 9.

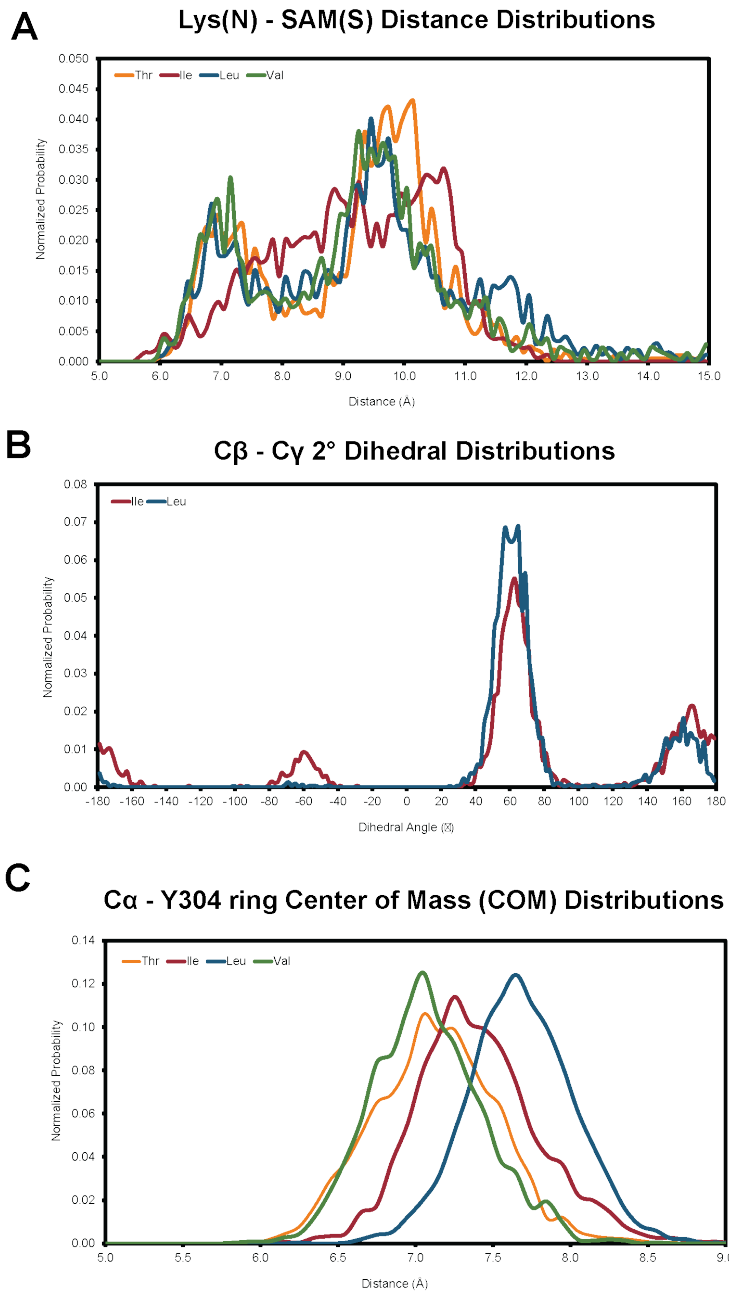


**Figure S3. Additional MSAD trajectory analyses of PRDM9 substrate selectivity.** A, Lys(N) - SAM(S) Distance Distributions. B, C $\beta$  - C $\gamma$  2° Dihedral Angle Distributions. C, C $\alpha$  - Y304 ring Center of Mass (COM) Distance Distributions.

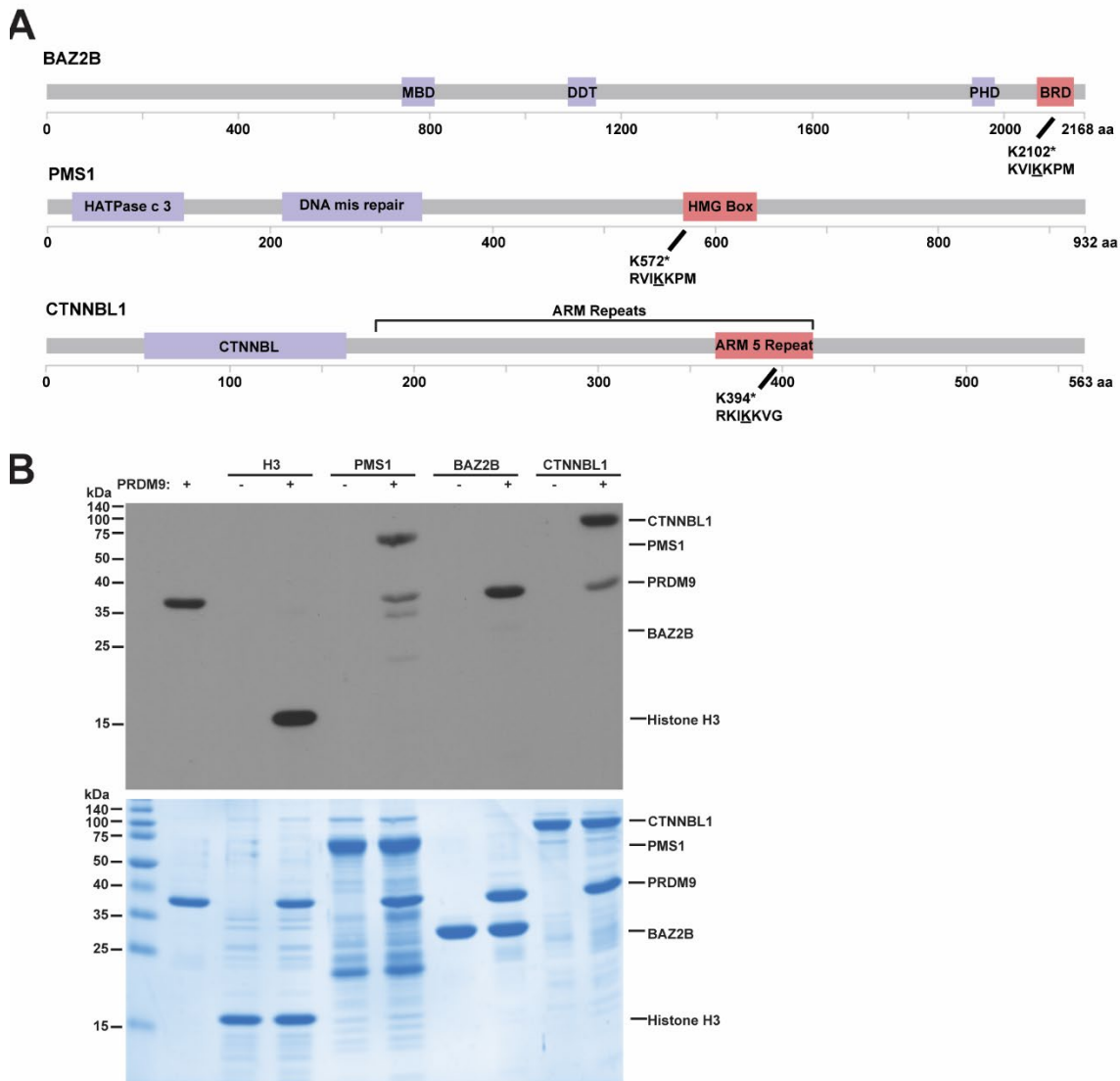


**Figure S4. Domain maps of putative PRDM9 non-histone substrates and *in vitro* methyltransferase assays using recombinant proteins.** *A*, The predicated PRDM9 methylation site and 7-mer motif is displayed. Data for domain boundaries was derived from UniProt. *B*, PRDM9 activity on recombinant non-histone substrates detected by fluorography (top panel). Bottom panel shows total protein stained with Coomassie after separation by SDS-PAGE. Representative of two independent experiments.